New insight in the template decomposition process of large zeolite ZSM-5 crystals: An in situ UV-Vis/fluorescence micro-spectroscopy study

ARTICLE *in* PHYSICAL CHEMISTRY CHEMICAL PHYSICS · MARCH 2011

Impact Factor: 4.49 · DOI: 10.1039/c0cp02220a · Source: PubMed

2 AUTHORS, INCLUDING:

Bert M Weckhuysen
Utrecht University
595 PUBLICATIONS **16,731** CITATIONS

SEE PROFILE

PCCP

View Online
Dynamic Article Links

Cite this: *Phys. Chem. Chem. Phys.*, 2011, **13**, 3681–3685

www.rsc.org/pccp

PAPER

New insight in the template decomposition process of large zeolite ZSM-5 crystals: an *in situ* UV-Vis/fluorescence micro-spectroscopy study

Lukasz Karwacki and Bert M. Weckhuysen*

Received 20th October 2010, Accepted 22nd November 2010
DOI: 10.1039/c0cp02220a

A combination of *in situ* UV-Vis and confocal fluorescence micro-spectroscopy was used to study the template decomposition process in large zeolite ZSM-5 crystals. Correlation of polarized light dependent UV-Vis absorption spectra with confocal fluorescence emission spectra in the 400–750 nm region allowed extracting localized information on the nature and amount of chemical species formed upon detemplation at the single particle level. It has been found by means of polarized light dependent UV-Vis absorption measurements that the progressive growth of molecules follows the orientation of the straight channels of ZSM-5 crystals. Oligomerizing template derivatives lead to the subsequent build-up of methyl-substituted benzenium cations and more extended coke-like species, which are thermally stable up to ~740 K. Complementary confocal fluorescence emission spectra showed nearly equal distribution of these molecules within the entire volume of the thermally treated zeolite crystals. The strongest emission bands were appearing in the orange/red part of the visible spectrum, confirming the presence of large polyaromatic molecules.

1. Introduction

The hydrothermal synthesis of zeolites often requires a structure-directing molecule to ensure the assembly of their long-range highly ordered structure. The template molecules have to be removed from the zeolite framework to allow the accessibility of the micropores formed. To do so, zeolite crystals are most commonly thermally detemplated in an oxidative (calcination) or inert (pyrolysis) atmosphere.[1–4]

Many attempts have been made to unravel the mechanism of the template decomposition process in MFI-type zeolite crystals using bulk techniques, such as nitrogen sorption,[5] gas chromatography,[3] thermoanalytical techniques,[1,6–8] X-ray powder diffraction[8,9] and mass spectrometry.[10] Unfortunately, as the chemical information of the detemplation process of zeolites is averaged over the whole sample volume, more detailed, spatially resolved approaches have to be called in. Few successful attempts in this direction involve optical, fluorescence and IR microscopy, which gave new insight into the template decomposition process.[5,7,11,12] Nevertheless, no *in situ* attempts of relating the chemical information of the template derivatives to the internal architecture of MFI-type materials has yet been made.

Here, we report on an experimental approach combining UV-Vis and confocal fluorescence micro-spectroscopy to map *in situ* the template decomposition process in large zeolite ZSM-5 crystals. Correlation of polarized light dependent UV-Vis absorption spectra with fluorescence emission spectra in the 400–750 nm region leads to localized chemical information on the origin and nature of template derivatives during realistic detemplation conditions.

Inorganic Chemistry and Catalysis, Debye Institute for Nanomaterials Science, Utrecht University, Sorbonnelaan 16, 3584 CA Utrecht, The Netherlands. E-mail: b.m.weckhuysen@uu.nl; Fax: +31 30 251 1027

2. Experimental

2.1 UV-Vis spectroscopy measurements

UV-Vis spectroscopy studies were performed using an Olympus BX41M upright research microscope provided with a 50 × 0.5 NA objective lens. Illumination of the sample was performed using a 75 W Tungsten lamp. The microscopy setup was equipped with a 50/50 double-viewport tube, which accommodated a CCD video camera (ColorView IIIu, Soft Imaging System GmbH) and an optical fibre mount. The microscope was connected to a CCD UV-Vis spectrometer (AvaSpec-2048TEC, Avantes) by a 200 μm-core fibre. UV-Vis spectroscopy measurements were performed using an *in situ* cell (Linkam Scientific Instruments FTIR 600) equipped with a temperature controller (Linkam Scientific Instruments TMS 94). Spectra were collected every 30 s since the start of the experiment. A rotatable polarizer was introduced between the objective lens and detector to separate the desirable light polarization.

ZSM-5 crystals with dimensions of 100 × 20 × 20 μm and a Si/Al ratio of ~17 were provided by ExxonMobil, Machelen, Belgium. The raw materials for the synthesis of these ZSM-5

crystals were (1) Ludox AS40, (2) TPABr (Fluka), (3) $Al_2(SO_4)_3 \cdot 18H_2O$ (Baker) and (4) NH_4OH (29%), with molar compositions of 6.65 $(NH_4)_2O$/0.67 TPA_2O/0.025 Al_2O_3/10 SiO_2/121 H_2O. For synthesis, (1) and (2) were mixed, subsequently (3) was added and mixed for 5 min, followed by addition of (4) and mixing for ~7 min. Heating was carried out 2 h to 453 K (7 days soak time under static conditions), followed by washing and drying at 393 K for 12 h.

2.2 Confocal fluorescence micro-spectroscopy

The confocal fluorescence micro-spectroscopy set-up was based on an ECLIPSE 90i upright microscope with a 50 × 0.55 NA dry objective. Measurements were performed using a Linkam FTIR 600 *in situ* spectroscopic cell mounted to the confocal fluorescence microscope. The samples were heated to 550 K with a ramp of 15 K min^{-1} and then to the final temperature (670 K, 700 K, 740 K, 760 K, 780 K and 800 K) with a rate of 5 K min^{-1} under a N_2 stream (20 ml min^{-1}). After achieving the desired temperature, samples were immediately cooled to room temperature. Confocal fluorescence emission spectra were acquired with a Nikon A1 Confocal Laser Microscope System equipped with six laser lines (405 nm, 457 nm, 488 nm, 514 nm, 561 nm and 640 nm). The emission spectra were detected with 32 channels detector in the range 420–500, 470–550, 505–585, 530–610, 575–655 and 655–735 nm for the six laser lines, respectively. The collected emission spectra overlap allowing their normalization and stitching into a single spectrum in the approximate range 400–750 nm. Full stacks of the confocal fluorescence slices were used to obtain the spectral information from the entire crystal volume.

3. Results and discussion

To better understand the mechanism of zeolite ZSM-5 detemplation and connect it to information obtained during the *in situ* spectroscopic studies on template removal, Fig. 1 illustrates the degradation of tetrapropylammonium (TPA) and the mechanism of the template derivatives development.

Two gradual template decomposition steps have been proposed.[2,13] At low temperature a Hofmann elimination of TPA to tripropylamine (Pr_3N) and propene (Fig. 1a(1)) occurs. In a second step the degradation of Pr_3N to lower amines and consequently to propene is possible *via* β-elimination. Finally,

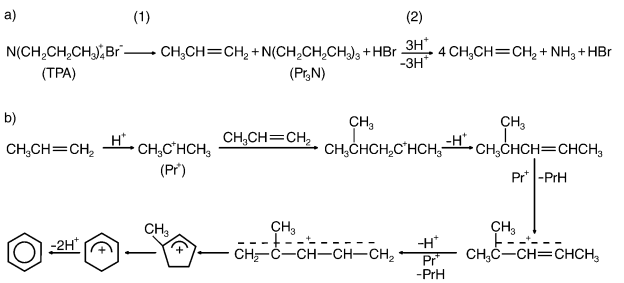

Fig. 1 (a) Simplified mechanism of tetrapropylammonium template degradation within ZSM-5 zeolite crystals. (b) Simplified mechanism of propene-to-aromatics conversion occurring during detemplation of ZSM-5 crystals.

the unsaturated products undergo oligomerization, cyclization and aromatization leading to the gradual increase in the molecular size and aromaticity.[14] In addition, from studies of Mores *et al.*[15] it becomes apparent that increasing the molecular size leads to generation of polymethylated aromatic species and consequently coke-like molecules. This is in line with Bilger *et al.* reporting on the generation of molecules like toluene, mesitylene, naphthalene and bigger[3] and leads us to expect an intense blackening of the ZSM-5 crystal upon detemplation.

In a first set of experiments as-prepared ZSM-5 crystals were thermally treated in the *in situ* reaction cell. From a previous study it is evident that large zeolite materials are not single crystals, but consist of different subunits.[16] In case of the ZSM-5 crystals under investigation two different regions of micropores orientation can be distinguished.[17,18] This is illustrated in Fig. 2, where a schematic representation of an individual ZSM-5 crystal is shown based on the results proposed by Karwacki *et al.*[17] The orange regions represent the areas of the crystal where straight channels are perpendicular and open to the surface, whereas in the blue regions sinusoidal channels open to the surface can be found.

Two sets of zeolite crystals were studied with polarization dependent optical and UV-Vis absorption experiments. In both cases crystal's region A have been measured. First, light polarization was set in the position I (indicating a 90° rotation between the straight channels parallel to the ZSM-5 crystal surface). In the second experiment the light polarization direction (II) was aligned with the straight channels of ZSM-5 (Fig. 2). Upon thermal treatment optical images of the crystals under study have been collected. This is shown in Fig. 3a and c.

Upon detemplation both ZSM-5 crystals start to be colored at ~670 K. Continued heating of crystal I (Fig. 3a) leads to a significant darkening at approximately 760 K, with a maximum around 780 K, indicating an increase in the oligomerization/aromatization of the template derivatives.[3] After ~45 min at 800 K the crystal appears less colored, which is caused by the thermal breakdown of the coke-like molecules. Observations of the darkening of crystal I are accompanied by polarized light UV-Vis absorption spectra (Fig. 3b), where it was found that after 15 min at 800 K a broad UV-Vis absorption band with the maximum at 410 nm extends to the visible region of the electromagnetic spectrum.

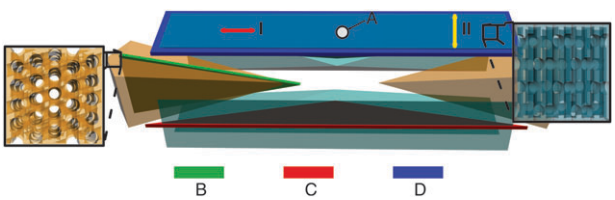

Fig. 2 3-D representation of an individual ZSM-5 zeolite crystal indicating crystal's tip and main body areas. Pore orientations vary; straight channels are open to the surface in the crystal tip (orange areas), while the blue area of the body has sinusoidal channels opened to the surface. Indicators I and II denote the light polarization direction during the UV-Vis absorption measurements. Four examined areas A–D are explained in the remainder of the text.

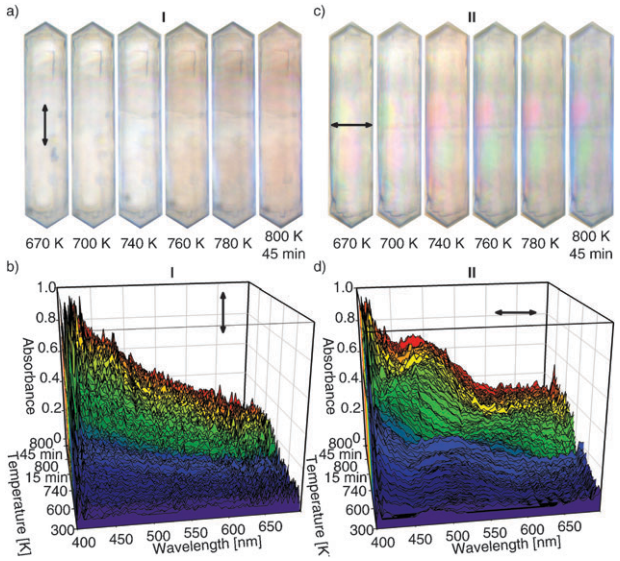

Fig. 3 (a) Optical images of the ZSM-5 crystals upon thermal treatment. Light is polarized in the direction I shown in Fig. 2. (b) Complementary time-resolved UV-Vis absorption spectra recorded during the detemplation of ZSM-5 crystal, shown in a. (c) and (d), same as a and b, but for a second ZSM-5 crystal. Light is polarized in the direction II.

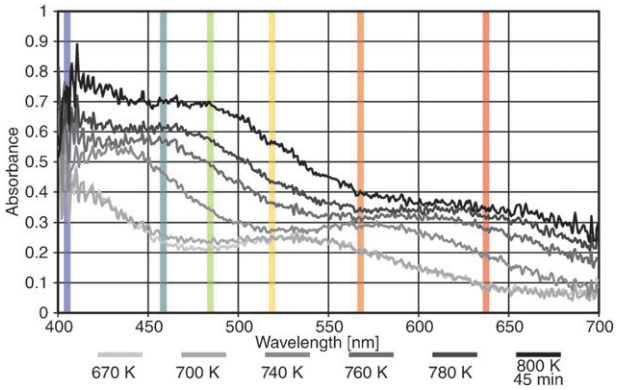

Fig. 4 UV-Vis absorption spectra recorded during the detemplation of crystal II (light polarization direction follows direction of the straight channels), at temperatures in which optical images have been collected. The vertical lines at 405, 457, 488, 514, 561 and 640 nm indicate six laser lines used for the acquisition of confocal fluorescence spectra in the 400–750 nm region.

In contrast, the optical images collected from crystal II (polarized light in the direction parallel to the ZSM-5 straight channels) appear different (Fig. 3c). The coloration of the crystal already appears at ~740 K and is followed by an intense blackening of the crystal. Surprisingly, even after 45 min at 800 K the coloration of the crystal increases. This suggests that the molecules generated in the straight channels of ZSM-5 are more resistant towards thermal breakdown. The UV-Vis absorption spectra of crystal II reveal a strong dependency between the polarized light and the molecules aligned in the straight channels of ZSM-5 (Fig. 3d). In order to closely inspect the spectral changes of crystal II under study Fig. 4 shows the UV-Vis absorption spectra at distinct temperatures at which optical images were collected (Fig. 3b).

The spectra in Fig. 4 reveal more detailed information on the nature of the template decomposition in the straight channels of ZSM-5. An absorption band at ~410 nm is present (Fig. 3d) similarly to the one found for crystal I (Fig. 3b). From the numerous spectroscopic studies on the unsaturated carbenium ions in zeolites it is apparent that the absorption band around 410 nm belongs to the π–π* transitions in methyl-substituted benzenium cations.[19–21] This assignment is in line with the molecular growth mechanism shown in Fig. 1b and leads us to expect further increase in the molecular sizes and a rise of the more extended conjugated aromatic species leading to the red shift in the optical absorption region. Indeed, at approximately 550 K (~20 min of detemplation) an absorption band at 500 nm emerges. Upon a temperature increase to ~700 K, the band intensity is boosted and the band maximum shifted to approximately 530 nm and at 740 K shifts further to the 570 nm position. At 670 K a third absorption band emerges at ~470 nm and gradually increases with the temperature of detemplation, while the 570 nm band visible at 740 K further shifts towards 620 nm at 800 K after 45 min, suggesting the generation of large aromatics.

No distinct absorption bands could be distinguished above 640 nm, suggesting that sizes of the molecules generated in the straight channels of ZSM-5 are partially hindered by the spatial constrains effect. This behavior is not uncommon for zeolite ZSM-5 and was previously reported by Kox *et al.*, Stavitski *et al.* and Buurmans *et al.* using styrene and thiophene compounds as spectroscopic probe molecules.[22–26]

As the observed UV-Vis absorption bands partially overlap and are highly influenced by background changes, additional information on the detemplation process of large ZSM-5 crystals has been obtained with confocal fluorescence micro-spectroscopy. Knowing that the detection limit of the fluorescence emission significantly exceeds UV-Vis absorption and that the obtained spectral information is complementary[27] an array of six laser lines was used to investigate the molecules formed within detemplated ZSM-5 crystals. The exact excitation wavelengths of lasers used for the confocal fluorescence micro-spectroscopy study are indicated in Fig. 4.

Combination of the 405, 457, 488, 514, 561 and 640 nm excitation lines with the adjustable detector array allows recording fluorescence emission spectra in the 400–750 nm region. This is shown in Fig. 5 where three different volumes of the ZSM-5 crystal were studied with the confocal fluorescence emission micro-spectrometer (regions B–D illustrated in Fig. 2).

The collected fluorescence emission spectra of volumes B–D (Fig. 5) indicate a nearly uniform character and distribution of the template derivatives generated within the different ZSM-5 crystal's volumes during the detemplation process. At the same temperatures the fluorescence emission spectra from different volumes are comparable, however, small variations in the spectral intensity are observed.

Almost no fluorescence is recorded at 670 K, which is in line with the optical images of the transparent ZSM-5 crystal in Fig. 3. The intensity of the broad emission band appearing at 610 nm at ~700 K is greatly enhanced at 740 K where two additional shoulders at 570 and 660 nm emerge. At this point fluorescence emission is maximal and a further increase of the

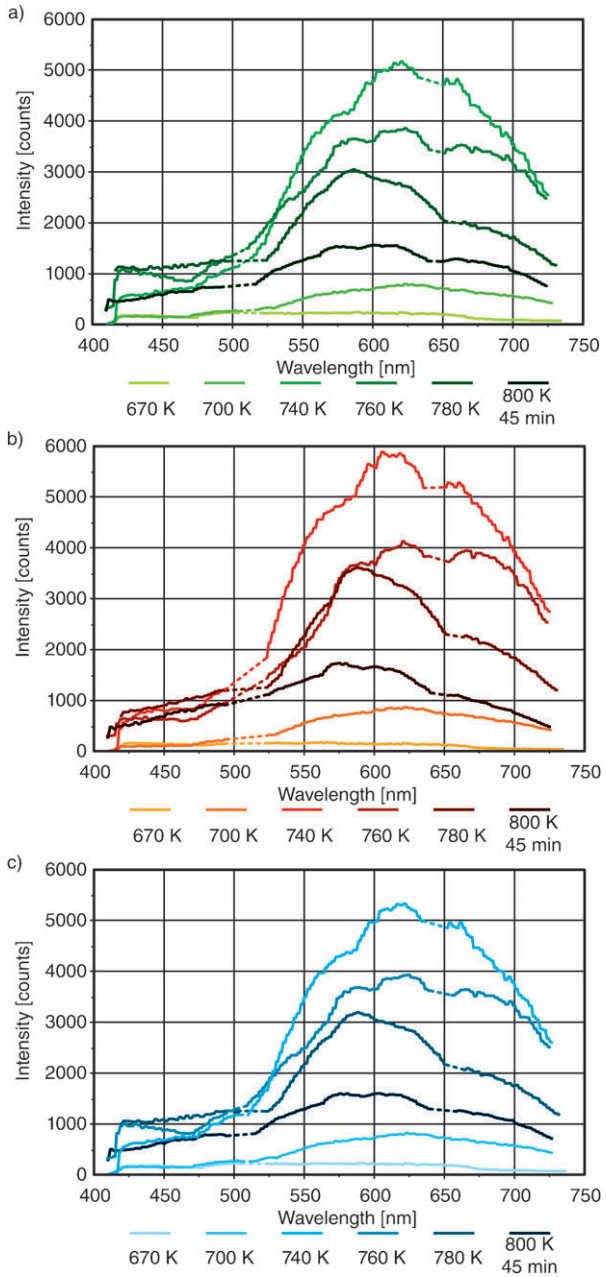

Fig. 5 (a) Fluorescence emission spectra of the template decomposition process in the ZSM-5 crystals recorded. The temperature dependent spectra are collected from the plane color-coded in green in Fig. 2 (region B). (b) and (c) same as a, but for the crystal planes indicated in Fig. 2 as red and blue, respectively. The darker the color of the spectra, the higher the temperature (or longer time) of the detemplation.

temperature (or time) causes decomposition of the previously generated template derivatives, which is followed by a decrease in the spectral intensity.

Comparison of Fig. 4 and 5, *i.e.* UV-Vis absorption and fluorescence emission spectra, shows the advantageous character of the approach. The UV-Vis absorption band visible at ~530 nm at 700 K is shifted in the emission spectrum to ~630 nm. Its further development to a 570 nm absorption band at 740 K (Fig. 4) is accompanied with the 580 nm shoulder appearing in the fluorescence emission band. Lastly, a distinct fluorescence emission band with maximum at 670 nm at 760 K (Fig. 5) may be connected to the development of a 470 nm UV-Vis absorption band (Fig. 4). It is important to stress the advantageous aspect of the remarkable sensitivity of the fluorescence emission spectroscopy. Here, the decrease of the amount of the template derivatives above 740 K is clearly visible, while the emerging background in the UV-Vis absorption spectra most probably obscures this observation.

To facilitate the understanding of the template derivatives distribution within the volume of the zeolite crystal, partially detemplated samples have been measured with confocal fluorescence microscopy upon thermal treatment. Fig. 6 illustrates the progress in the template derivatives formation/decomposition in an individual ZSM-5 crystal.

As prepared ZSM-5 zeolite crystals are colorless and non-fluorescent. Upon heating, weak UV-Vis absorption bands assigned to template derivatives oligomerization[3] start arising already below 500 K, accompanied by a weak fluorescence emission. The distinct fluorescence emission signals appear around 670 K in all 400–750 nm region and gradually increase in intensity up to 740 K, at which all examined detection regions indicate significant fluorescence. This points towards a variety of generated template derivatives. Further increase in the temperature shifts the highest emission signal from light blue/green towards orange/red part of the electromagnetic spectrum, suggesting a continued growth of coke-like molecules and leading to the formation of species, such as poly-substituted aromatics.[3] This is continued up to 780 K, where a further increase in the emission in the red part of the visible spectrum is observed. As the temperature increase

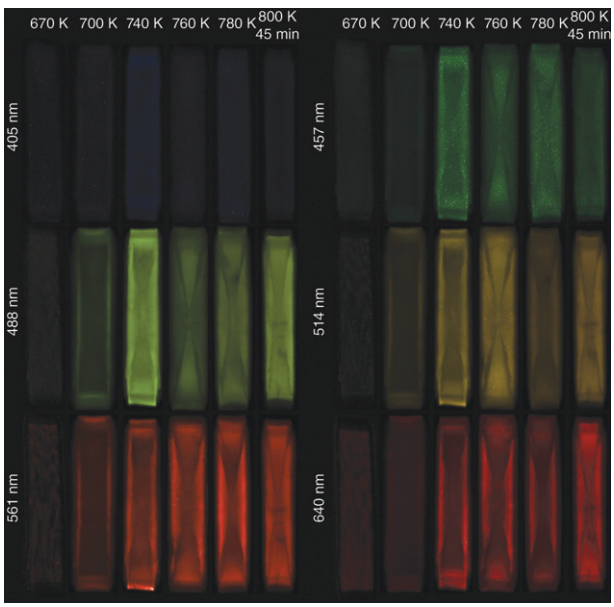

Fig. 6 Time evolution of the template decomposition process in ZSM-5 crystals as visualized by confocal fluorescence microscopy. With increasing temperature, the fluorescence intensity raises, shifts and eventually fades away. A set of six laser lines (405, 457, 488, 514, 561 and 640 nm) and detection channels (425–475, 475–515, 510–550, 525–575, 575–635 and 675–735 nm) was used. Pairs laser/detector are color-coded as blue, dark green, light green, orange, red and dark red, respectively. All crystal slices are collected at the crystal's middle depth.

promotes the growth of conjugated systems, while spatial constrains of the micropores partially limit it, a certain amount of molecules will decompose to smaller fractions resulting in the spectral shift towards the blue region of the spectrum. This is best observed at 800 K, where the contribution of the green/yellow part of the spectrum (510–575 nm) is more intense than the red region (575–735 nm).

Conclusions

In situ UV-Vis and confocal fluorescence micro-spectroscopy are powerful methods for the spatially resolved mapping of the template decomposition process in large ZSM-5 crystals. It has been evidenced that upon increasing the detemplation temperature methyl-substituted benzenium cations are being generated leading to large coke-like derivatives. Polarization dependent UV-Vis absorption spectra revealed a significant accumulation of the large poly-substituted aromatics within the straight channels of ZSM-5. Moreover, the correlation between polarization dependent UV-Vis absorption measurements and localized confocal fluorescence emission spectral analysis unraveled the uniform detemplation within the volume of individual ZSM-5 crystals, as well as the temperature influence on the varying sizes of generated molecules. The appearance of small differences in the diffusion rate of the generated molecules studied by confocal fluorescence microscopy of a porous catalyst body allowed visualization of the internal architecture and molecular diffusion barrier of zeolite crystals as well as further confirmed the presence of a 90° intergrowth structure within large ZSM-5 crystals.

Acknowledgements

Dr Machteld Mertens (ExxonMobil, Machelen, Belgium) is kindly acknowledged for providing the as-prepared ZSM-5 crystals. Dr Eli Stavitski (Utrecht University) is recognized for writing the UV-Vis absorption measurements macro.

References

1 M. Soulard, S. Bilger, H. Kessler and J. L. Guth, *Zeolites*, 1987, **7**, 463–470.
2 L. M. Parker, D. M. Bibby and J. E. Patterson, *Zeolites*, 1984, **4**, 168–174.
3 S. Bilger, M. Soulard, H. Kessler and J. L. Guth, *Zeolites*, 1991, **11**, 784–791.
4 V. R. Choudhary and S. D. Sansare, *J. Therm. Anal.*, 1987, **32**, 777–784.
5 O. Pachtova, M. Kocirik, A. Zikanova, B. Bernauer, S. Miachon and J. A. Dalmon, *Microporous Mesoporous Mater.*, 2002, **55**, 285–296.
6 K. H. Gilbert, R. M. Baldwin and J. D. Way, *Ind. Eng. Chem. Res.*, 2001, **40**, 4844–4849.
7 I. Jirka, P. Sazama, A. Zikánová, P. Hrabánek and M. Kocirik, *Microporous Mesoporous Mater.*, 2011, **137**, 8–17.
8 M. Milanesio, G. Artioli, A. F. Gualtieri, L. Palin and C. Lamberti, *J. Am. Chem. Soc.*, 2003, **125**, 14549–14558.
9 M. L. Gualtieri, A. F. Gualtieri and J. Hedlund, *Microporous Mesoporous Mater.*, 2006, **89**, 1–8.
10 X. T. Gao, C. Y. Yeh and P. Angevine, *Microporous Mesoporous Mater.*, 2004, **70**, 27–35.
11 Y. S. Lin, N. Yamamoto, Y. Choi, T. Yamaguchi, T. Okubo and S. I. Nakao, *Microporous Mesoporous Mater.*, 2000, **38**, 207–220.
12 E. Mateo, A. Paniagua, C. Guell, J. Coronas and J. Santamaria, *Mater. Res. Bull.*, 2009, **44**, 1280–1287.
13 E. R. Geus, J. C. Jansen and H. van Bekkum, *Zeolites*, 1994, **14**, 82–88.
14 M. L. Poutsma, in *Zeolite Chemistry and Catalysis*, ed. J. A. Rabo, ACS Monograph 171, Washington, DC, 1976, p. 437.
15 D. Mores, E. Stavitski, M. H. F. Kox, J. Kornatowski, U. Olsbye and B. M. Weckhuysen, *Chem.–Eur. J.*, 2008, **14**, 11320–11327.
16 L. Karwacki, E. Stavitski, M. H. F. Kox, J. Kornatowski and B. M. Weckhuysen, *Angew. Chem., Int. Ed.*, 2007, **46**, 7228–7231.
17 L. Karwacki, M. H. F. Kox, D. A. M. de Winter, M. R. Drury, J. D. Meeldijk, E. Stavitski, W. Schmidt, M. Mertens, P. Cubillas, N. John, A. Chan, N. Kahn, S. R. Bare, M. Anderson, J. Kornatowski and B. M. Weckhuysen, *Nat. Mater.*, 2009, **8**, 959–965.
18 E. Stavitski, M. R. Drury, D. A. M. de Winter, M. H. F. Kox and B. M. Weckhuysen, *Angew. Chem., Int. Ed.*, 2008, **47**, 5637–5640.
19 I. Kiricsi, H. Forster, G. Tasi and J. B. Nagy, *Chem. Rev.*, 1999, **99**, 2085–2114.
20 M. Bjørgen, S. Svelle, F. Joensen, J. Nerlov, S. Kolboe, F. Bonino, L. Palumbo, S. Bordiga and U. Olsbye, *J. Catal.*, 2007, **249**, 195–207.
21 M. Bjørgen, F. Bonino, S. Kolboe, K.-P. Lillerud, A. Zecchina and S. Bordiga, *J. Am. Chem. Soc.*, 2003, **125**, 15863–15868.
22 M. H. F. Kox, E. Stavitski and B. M. Weckhuysen, *Angew. Chem., Int. Ed.*, 2007, **46**, 3652–3655.
23 E. Stavitski, M. H. F. Kox and B. M. Weckhuysen, *Chem.–Eur. J.*, 2007, **13**, 7057–7065.
24 M. H. F. Kox, A. Mijovilovich, J. Sattler, E. Stavitski and B. M. Weckhuysen, *ChemCatChem*, 2010, **2**, 564–571.
25 M. H. F. Kox, K. F. Domke, J. P. R. Day, G. Rago, E. Stavitski, M. Bonn and B. M. Weckhuysen, *Angew. Chem., Int. Ed.*, 2009, **48**, 8990–8994.
26 I. L. C. Buurmans, E. A. Pidko, J. M. de Groot, E. Stavitski, R. A. van Santen and B. M. Weckhuysen, *Phys. Chem. Chem. Phys.*, 2010, **12**, 7032–7040.
27 J. R. Lakowicz, *Principles of Fluorescence Spectroscopy*, Springer, New York, 2006.